Available online at www.sciencedirect.com
ScienceDirect
Wear 263 (2007) 501–507
WEAR
www.elsevier.com/locate/wear

Nanofretting behaviors of NiTi shape memory alloy

Linmao Qian [a], Zhongrong Zhou [a,*], Qingping Sun [b], Wenyi Yan [c]

[a] *Tribology Research Institute, National Traction Power Laboratory, Southwest Jiaotong University, Chengdu 610031, China*
[b] *Department of Mechanical Engineering, The Hong Kong University of Science and Technology, Hong Kong, China*
[c] *School of Engineering and Information Technology, Deakin University, Geelong, Vic. 3217, Australia*

Received 4 August 2006; received in revised form 15 December 2006; accepted 18 December 2006
Available online 23 May 2007

Abstract

Nanofretting refers to cyclic movements of contact interfaces with the relative displacement amplitude at the nanometer scale, where the contact area and normal load are usually much smaller than those in fretting. Nanofretting widely exists in microelctromechanical systems (MEMS) and may become a key tribological concern besides microwear and adhesion. With a triboindenter, the nanofretting behaviors of a nickel titanium (NiTi) shape memory alloy are studied under various normal loads (1–10 mN) and tangential displacement amplitudes (2–500 nm) by using a spherical diamond tip. Similar to fretting, the nanofretting of NiTi/diamond pair can also be divided into different regimes upon various shapes of tangential force–displacement curves. The dependence of nanofretting regime on the normal load and the displacement amplitude can be summarized in a running condition nanofretting map. However, due to the surface and size effects, nanofretting operates at some different conditions, such as improved mechanical properties of materials at the nanometer scale, small apparent contact area and single-asperity contact behavior. Consequently, different from fretting, nanofretting was found to exhibit several unique behaviors: (i) the maximum tangential force in one cycle is almost unchanged during a nanofretting test, which is different from a fretting test where the maximum tangential force increases rapidly in the first dozens of cycles; (ii) the tangential stiffness in nanofretting is three orders magnitude smaller than that in fretting; (iii) the friction coefficient in nanofretting is much lower than that in fretting in slip regime; (iv) no obvious damage was observed after 50 cycles of nanofretting under a normal load of 10 mN.

Keywords: Nanofretting; Nickel titanium shape memory alloy; Fretting; Friction

1. Introduction

It is well known that sliding, rolling and fretting are three basic modes of tribological movement between two contact surfaces [1–2]. With the rapid development in nano science and technology, nanofretting, as a new tribological movement mode, was proposed recently [3]. Nanofretting refers to cyclic movements of contact interfaces with the relative displacement amplitude in nanometer scale, where the contact area and normal load are usually much smaller than those in fretting. As nanofretting widely exists in microelectromechanical systems (MEMS), it may damage the contact surfaces and sometimes induce the failure of micro devices in MEMS. Therefore, with the development in MEMS, nanofretting damage may become a key tribological concern besides microwear and adhesion.

Nanofretting usually appears in MEMS with cyclic movements, such as micropump, microvalve, microswitch, micromotor, and so on, where the contact surfaces may sustain an alternating stress. Since the surface forces, such as adhesion and friction force, may play dominant roles compared to bulk forces in MEMS, the chemical and physical behaviors of the contact surfaces may show a strong effect on the mechanism of nanofretting [4,5]. Compared to multi-asperities contact in fretting, the contact in nanofretting is usually in single-asperity contact. Therefore, due to the surface and size effects, nanofretting should not be simply considered as an extension of fretting from micrometer to nanometer scale. Rather nanofretting may exhibit its unique behaviors either in running property or damage mechanism.

The earliest research relative to nanofretting can be traced back to the work by Kennedy et al. in 1980s [6]. While conducting fretting experiments, they found that the damage initiated on the steel surface at a load of 60 N and a tangential displacement amplitude of 60 nm. More recently, Varenberg et al. [7] reported

* Corresponding author. Tel.: +86 28 87600971; fax: +86 28 87603142.
E-mail address: zrzhou@home.swjtu.edu.cn (Z. Zhou).

0043-1648/$ – see front matter © 2007 Elsevier B.V. All rights reserved.
doi:10.1016/j.wear.2006.12.045

the nano scale fretting tests of a silica microsphere with 3.1 μm in diameter against silicon flat specimen by an atomic force microscope (AFM). So far, the behaviors of nanofretting are still far from being understood.

Because of its well-known superelastic and shape memory effect, NiTi shape memory alloy (SMA) has been proposed as sensors as well as large-strain actuators in MEMS [8]. Thus, understanding and control of the nanofretting behaviors of NiTi SMA becomes an important issue of concern. In this paper, tangential nanofretting experiments are conducted on a NiTi SMA by using a triboindenter. The running properties and damage behaviors of nanofretting are reported. The effects of normal load, displacement amplitude and nanofretting cycle on the behaviors of nanofretting are discussed, where the distinctions between nanofretting and fretting are emphasized.

2. Materials and testing methods

Commercial 0.5 mm-thick NiTi polycrystalline cold-rolling sheets were purchased from Shape Memory Applications, Inc., USA. The nominal alloy composition is Ni-50.7 and Ti-49.3 in at.%. The grain size of the NiTi sheet is about 50–100 nm as observed by a transmission electron microscopy [9]. With a differential scanning calorimeter, the characteristic transformation temperatures, namely R_s, R_f (rhombohedral phase start and finish temperatures on cooling), M_s, M_f (martensite start and finish temperatures on cooling), A_s and A_f (austenite start and finish temperatures on heating) were measured at heating and cooling rates of 1 °C/min and are listed in Table 1. Before the tests, the NiTi sheet was first cooled down in liquid nitrogen for 1 h and then heated up to 20 °C so that it is in martensite phase and shows shape memory effect at room temperature.

To characterize the mechanical properties of NiTi, tensile tests of sheet samples were performed by a universal testing machine with a temperature chamber. As shown in Fig. 1, the NiTi shows typical shape memory effect at temperatures below 40 °C, where it experiences two stages of deformation during loading process: martensite elastic deformation and martensite reorientation. Because of its shape memory effect, the residual deformation can be totally recovered by heating above A_f (59 °C). In addition, superelastic behavior is observed in the tensile tests of NiTi at temperatures above 59 °C, where the NiTi alloys experiences elastic deformation of austenite, phase transition from austenite to martensite, and reorientation plus elastic deformation of the martensite during the loading process. Due to the superelastic nature of the NiTi, both the elastic and phase transition deformations will recover during unloading.

Table 1
Phase transformation temperatures and room temperature structure (SME NiTi)

A_s (°C)	21
A_f (°C)	59
R_s (°C)	50
R_f (°C)	27
M_s (°C)	2
M_f (°C)	−35
Room temperature structure	Martensite

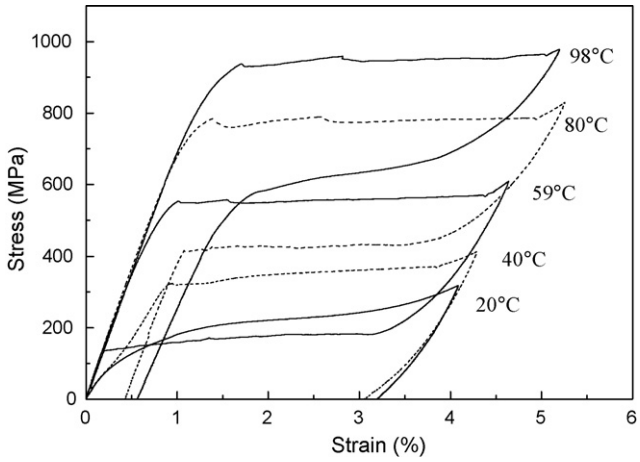

Fig. 1. The tensile stress–strain curves of NiTi at various temperatures.

The residual deformation at 80 and 98 °C mainly comes from the plastic yield of austenite and martensite [10]. Compression tests give similar curves except with a higher martensite reorientation stress or phase transition stress [11].

To prepare the samples for nanofretting tests, NiTi plates were cut into 10 mm × 10 mm pieces by a wire-cutting machine. Silicon carbon and aluminum oxide sand papers of various grades were used to polish the NiTi plate surfaces until a satisfactory surface quality was obtained. The final root-mean-square roughness of the specimens (over a 10 μm × 10 μm area) is about 5 nm measured by an atomic force microscope (AFM).

The nanofretting tests were run on the polished NiTi plates by a triboindenter at 60 °C, at which temperature the NiTi exhibits superelastic behavior (Fig. 1). The indenter is a spherical diamond tip with a cone angle of 60° and a nominal radius of 50 μm as shown in Fig. 2. In the tests, the normal load and the tangential displacement amplitude were varied. Four loads were chosen from 1 to 10 mN. Under each load, the nanofretting tests of NiTi were performed at eight different displacement amplitudes D between 2 and 500 nm. The same frequency of 0.05 Hz was used in all the tests. All experiments were performed under unlubricated condition and a relative humidity of 50–60%. In each case, the nanofretting test was repeated at least twice to

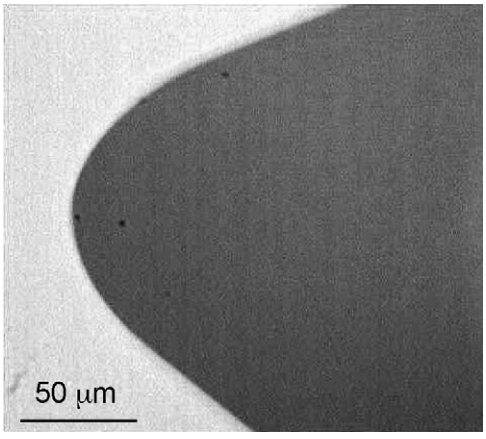

Fig. 2. The image of the spherical diamond indenter used in tangential nanofretting tests. The cone angle is 60° and the nominal radius is 50 μm.

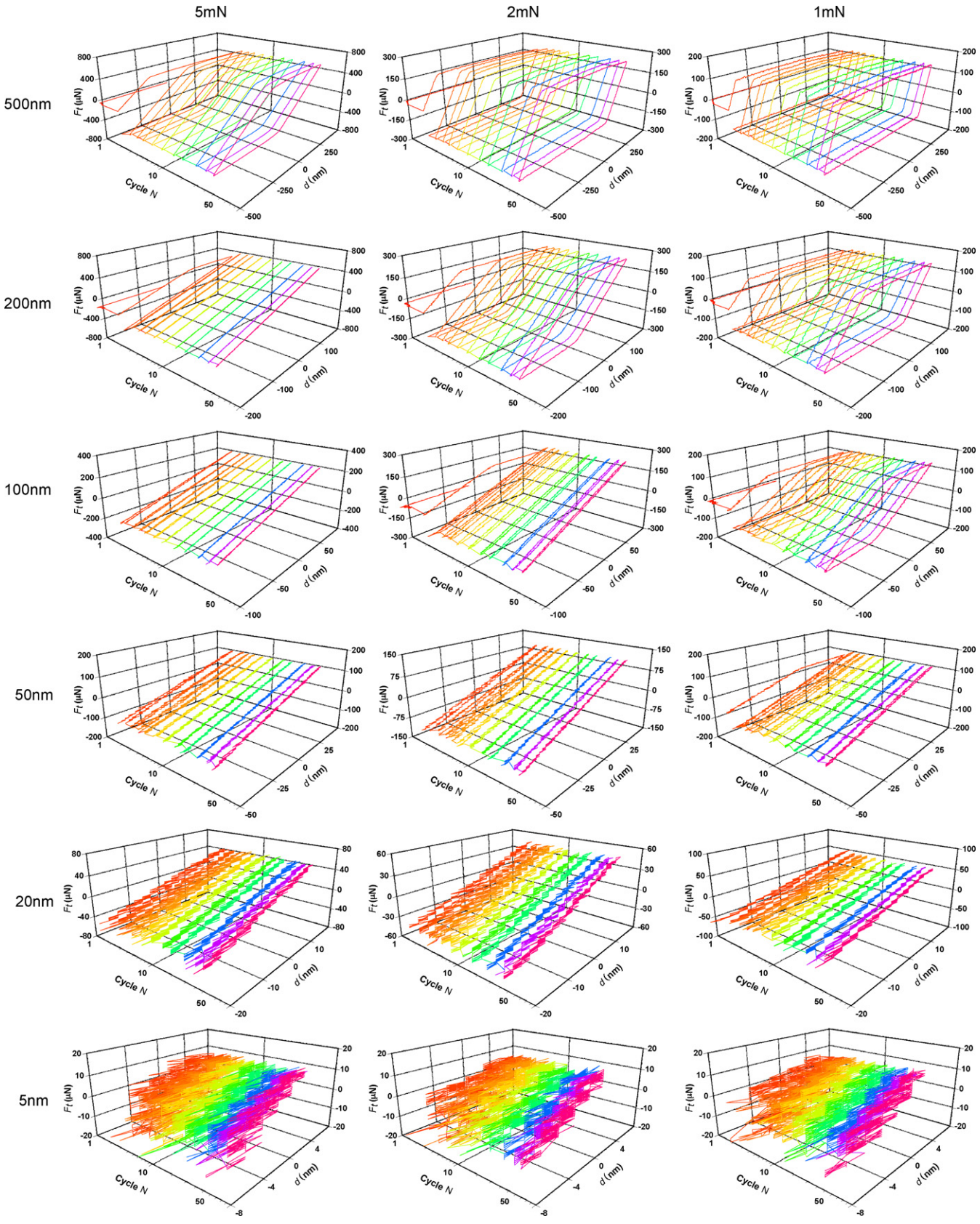

Fig. 3. The frictional logs (variation of the tangential force F_t and displacement d with number of nanofretting cycles N, or F_t–d–N curves) of NiTi/diamond pair corresponding to loads $F_n = 5$ mN, 2 mN and 1 mN and various displacement amplitudes D. $T = 60\,^{\circ}C$.

ensure the repetition of the results. After the tests, the topography of the wear area was characterized by an in situ atomic force microscope.

3. Results and discussions

Fig. 3 shows the frictional logs (variation of the tangential force F_t and displacement d with number of cycles N, or F_t–d–N curves) of NiTi against diamond indenter (or NiTi/diamond) corresponding to three normal loads $F_n = 5$ mN, 2 mN and 1 mN and various displacement amplitudes D. Similar to fretting, the nanofretting may also be divided into different regimes upon the shapes of F_t–d curves [12]. However, quite different from fretting, some unique behaviors are found in the nanofretting F_t–d–N curves of NiTi/diamond pair: (i) the maximum tangential force in one cycle is almost unchanged during a nanofretting test, which is different from a fretting test where the maximum tangential force increases rapidly in the first dozens of cycles; (ii) the tangential stiffness in nanofretting is three orders magnitude smaller than that in fretting; (iii) in slip regime, the friction coefficient in nanofretting is much lower than that in fretting. These behaviors are discussed below in detail.

To understand the dependence of the nanofretting regime on the normal load F_n and the tangential displacement amplitude D, Fig. 4 plots a running condition nanofretting map of NiTi/diamond pair [13]. Here, the stick regime is identified corresponding to quasi-closed shape F_t–d curve, such as examples shown in Fig. 3 with $F_n = 2$ mN and $D \leq 50$ nm. The slip regime corresponds to parallelepipedic shape F_t–d curve, such as examples shown in Fig. 3 with $F_n = 2$ mN and $D \geq 200$ nm. Between the stick regime and the slip regime, there exists a transition regime, which covers the cases in Fig. 3 with $F_n = 2$ mN and $D = 100$ nm. As a comparison, the running condition fretting map of NiTi against GCr15 steel ball (with a radius $R = 20$ mm) is also plotted in Fig. 4 [12]. Clearly, the displacement amplitude D in fretting is normally in micrometer scale, where three

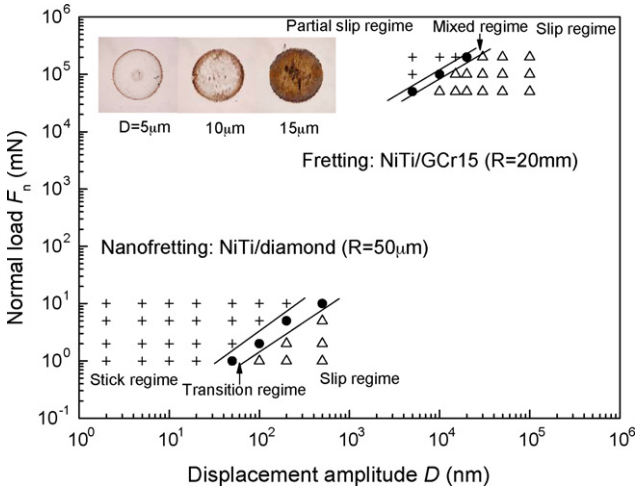

Fig. 4. The running condition nanofretting map of NiTi/diamond pair, compared with the running condition fretting map of NiTi/GCr15 pair. The up-left inset pictures show the wear scars on NiTi in fretting at $F_n = 50$ N with various values of D.

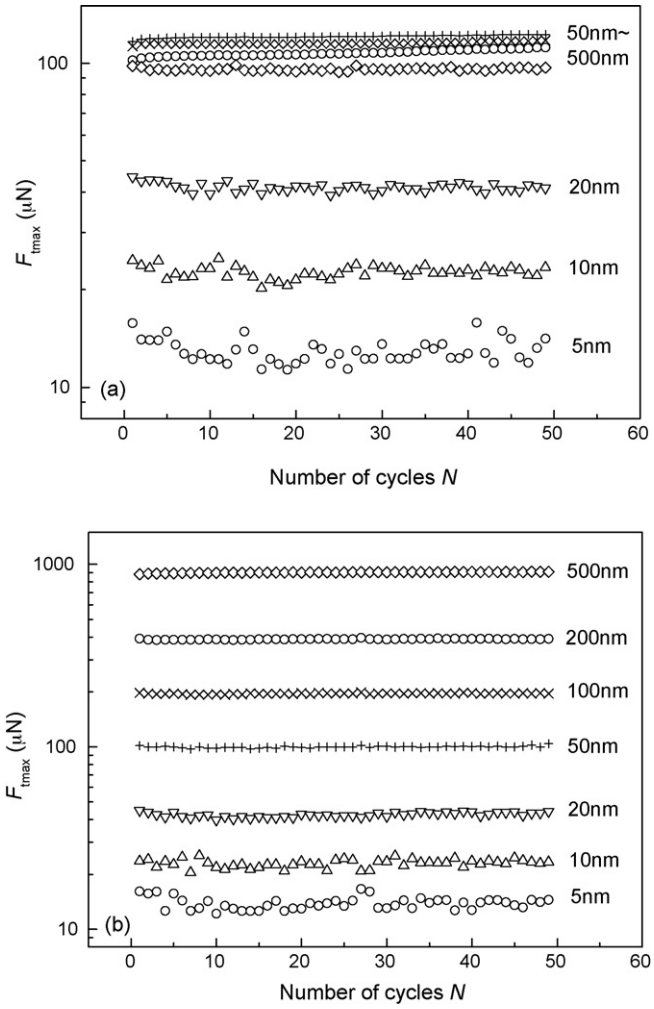

Fig. 5. The maximum tangential force F_{tmax} in a cycle vs. the number of nanofretting cycle N (F_{tmax}–N) curves of NiTi/diamond pair corresponding to various values of D for different normal loads F_n: (a) $F_n = 1$ mN; (b) $F_n = 10$ mN.

fretting regimes, namely partial slip regime, mixed regime and slip regime, are identified at various values of F_n and D. For NiTi/GCr15 pair at a F_n of 200 N, the fretting runs in partial slip regime at $D = 15$ μm, which indicates that the relative movement at an amplitude of 15 μm can be accommodated by the elastic deformation of system. The corresponding wear area consists of two parts: the adhesive zone in the center and the micro-slip zone around the edge. As the displacement amplitude D decreases, the micro-slip zone becomes narrow, see up-left inset in Fig. 4. Due to the difference in the operating conditions between nanofretting and fretting, the nanofretting runs in slip regime when D is as small as 100 nm at $F_n = 1$ mN. As F_n increases from 1 to 10 mN, the stick regime of nanofretting in the map expands from $D \leq 20$ to $D \leq 200$ nm. With the increase in D, a narrow transition regime with elliptic shape F_t–d curve is observed between stick regime and slip regime under various values of F_n.

To characterize the nanofretting kinetic behavior of NiTi/diamond pair, Fig. 5 shows the maximum tangential force F_{tmax} in a cycle versus the number of nanofretting cycle N (F_{tmax}–N) curves corresponding to various D for different normal load F_n. It is found that F_{tmax} almost keeps unchanged

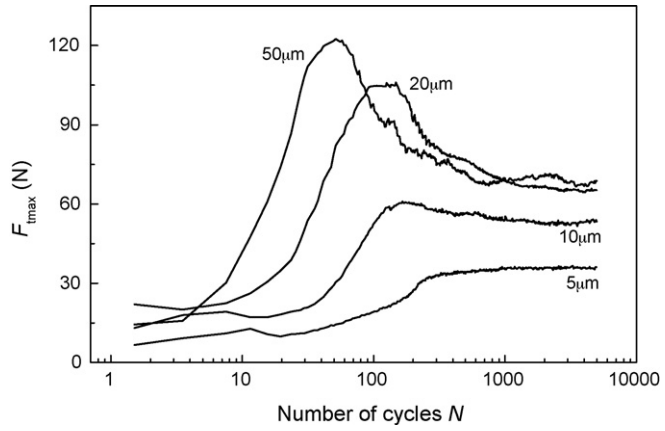

Fig. 6. The maximum tangential force F_{tmax} in a cycle vs. the number of fretting cycle N (F_{tmax}–N) curves of NiTi/GCr15 pair corresponding to various values of D for normal load $F_n = 100$ N.

with the increase in N for all the F_{tmax}–N curves under different normal loads and different tangential displacement amplitudes. These results are very different from those obtained in fretting tests of NiTi/GCr15 pair, where F_{tmax} increased during the first 50 cycles and then reached their maximum values, as shown in Fig. 6 [12]. The reason may be attributed to the difference in the contact conditions between nanofretting and fretting. Assuming linear elasticity without phase transition occurs before NiTi yields, the Hertzian contact area A and the maximum contact pressure p_0 in the contact area can be determined by [14]:

$$A = \pi\left(\frac{3F_n R}{4E}\right)^{2/3}, \quad (1)$$

$$p_0^3 = \frac{6F_n E^2}{\pi^3 R^2}. \quad (2)$$

Here, E is the effective elastic modulus of contact pairs. According to Eq. (1), the Hertzian contact area A of NiTi/GCr15 pair in fretting is estimated as 0.2–0.5 mm^2 for F_n between 50 and 200 N, which is about five orders larger than those of NiTi/diamond pair in nanofretting (2.3–10.9 μm^2 for F_n between 1 and 10 mN). As shown in Fig. 7, due to the size effect, the number of asperities in the contact area of fretting should be five orders more than that of nanofretting for NiTi plate with the same surface roughness. As a result, the contact in fretting should be a typical multi-asperity contact and the contact in nanofretting could be considered as a single-asperity contact.

For multi-asperity contact of NiTi/GCr15 pair in fretting, the asperities in contact are usually suffered from plastic deformation due to the high local contact pressure and the tangential

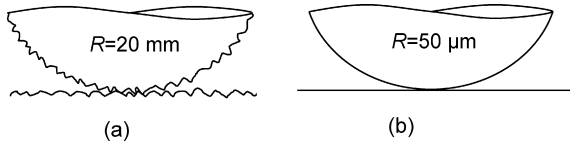

Fig. 7. The schematic illustration of the difference in the contact behavior between fretting and nanofretting: (a) the multi-asperity contact in fretting; (b) the single-asperity contact in nanofretting.

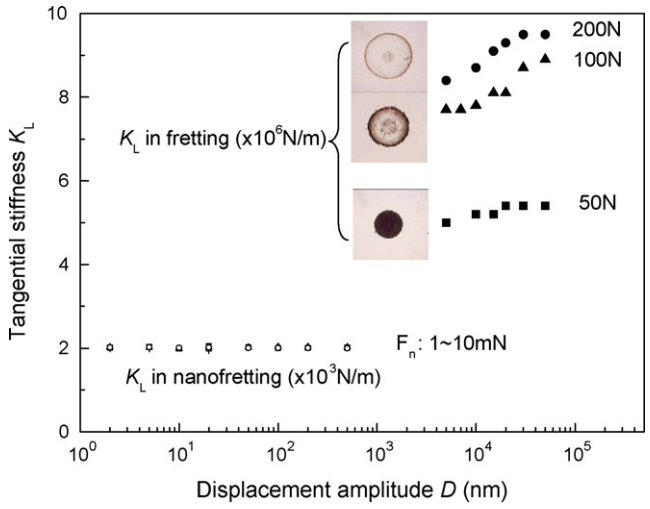

Fig. 8. The tangential stiffness K_L of NiTi/diamond pair in nanofretting at various loads plotted as the function of the displacement amplitudes D, compared with the results from NiTi/GCr15 pair in fretting. The inset pictures show the wear scars on NiTi in fretting at $D = 5$ μm with various values of F_n.

slip. Thus, the initial fretting cycles are more like a running-in process [15]. During the fretting process, the real contact area A_r will increase with the increase in the number of cycles [16]. The maximum tangential force F_{tmax} can be related to A_r by:

$$F_{tmax} = A_r S, \quad (3)$$

where S is the averaged shear stress over the real contact area A_r. In the present case of slip without obvious plastic deformation, S is equivalent to the shear strength of an adhesive junction and can be assumed to be independent on the contact pressure [17]. According to Eq. (3), F_{tmax} will then increase in the first 50 fretting cycles due to the increase in A_r.

However, for single-asperity contact of NiTi/diamond pair in nanofretting, the maximum contact pressure p_0 in the contact area is about 640–1378 MPa for various loads according to Eq. (2). The corresponding maximum shear stress beneath the contact surface is about 198–428 MPa [14]. On one hand, since all these values are below the martensite plastic shear strength of 800 MPa at 60 °C, no plastic deformation will occur during nanofretting. On the other hand, since the tensile phase transition stress of NiTi is 560 MPa at 60 °C as shown in Fig. 1, the corresponding tangential phase transition stress is about 280 MPa [11]. For $F_n = 5$ and 10 mN, as the maximum shear stress 339 and 428 MPa are higher than the tangential phase transition stress (280 MPa), the reversible phase transition deformation will arise in NiTi and the maximum shear stress will be limited to 280 MPa during nanofretting. Even though, without plastic deformation, the variation of the real contact area A_r for a single-asperity contact during a nanofretting process is negligibly small. Therefore, the tangential force F_{tmax} keeps a constant value during a nanofretting process.

In a nanofretting process, the part of the F_t–d curve of NiTi/diamond pair before gross slip is almost in a linear shape as shown in Fig. 3. Its slope in fact indicates the tangential stiffness K_L of the contact pair. As plotted in Fig. 8, the values of K_L in nanofretting (2000 N/m) are almost three orders

magnitude smaller than those of NiTi/GCr15 pair in fretting ($5–10 \times 10^6$ N/m). For a sphere/plane contact, the tangential stiffness K_L before slipping can be determined by the following function [14]:

$$K_L = 8a\left(\frac{2-v_1}{G_1} + \frac{2-v_2}{G_2}\right)^{-1}, \quad (4)$$

where G_i and v_i ($i=1,2$) are the shear modulus and Poisson ratio of the contact pairs, respectively. The contact area radius a in Eq. (4) is related to the normal load F_n by:

$$a = \left(\frac{3F_nR}{4E}\right)^{1/3}. \quad (5)$$

According to Eq. (4), the difference between the K_L in nanofretting and in fretting could be mainly attributed to the difference in the contact radius a in nanofretting (0.86–1.86 μm) and in fretting (0.25–0.40 mm). In addition, the variation of K_L in fretting might also be mainly induced by the variation of contact radius a, which increases with the normal load according to Eq. (5). The inset pictures in Fig. 8 shows the wear scars on NiTi at $D=5$ μm and at various loads, which clearly indicates that the K_L in fretting increases with the increase in contact radius a. Bear in mind that a large wear scar corresponds to a large contact area under the same fretting displacement amplitude.

Fig. 9 shows the friction coefficient f ($=F_t/F_n$) of NiTi/diamond pair in nanofretting as a function of the displacement amplitude D corresponding to various values of F_n. The f of NiTi/GCr15 pair in fretting is also plotted in Fig. 9 as a comparison. It is found that all the values of f of NiTi/diamond pair in nanofretting are between 0.09 and 0.12, which are about one-sixth of the values of f of NiTi/GCr15 pair in fretting [12]. Beside the difference in the ball materials, there might be three other reasons contributing to the different friction behaviors in fretting and in nanofretting [15]. First, compared to fretting, the small contact area in nanofretting reduces the number of particles trapped at the interface, and thus minimizes the plough contribution to the friction force. Second, when very low loads are used in microscale studies, the elastic modulus and nano-indentation hardness of materials are higher than their bulk values [15,18]. Since for the single-asperity contact in nanofretting, the friction coefficient f is related to the asperity radius R, the normal load

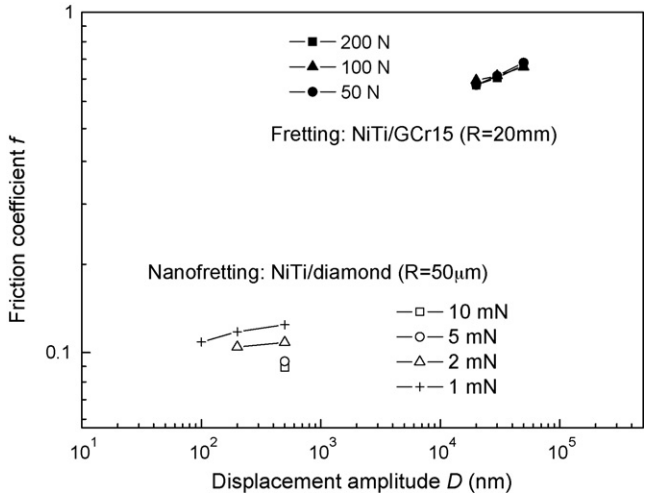

Fig. 9. The friction coefficient f of NiTi/diamond pair in nanofretting as the function of D at various loads, compared with the results from NiTi/GCr15 pair in fretting.

F_n and elastic modulus E by [17]:

$$f = \pi S\left(\frac{R}{E}\right)^{2/3} F_n^{-(1/3)}, \quad (6)$$

where S has the same meaning as in Eq. (3). The above equation suggests that f will decrease with the increase in the elastic modulus E. Thus, lack of plastic deformation and improved mechanical properties reduce the degree of wear and friction. Finally, the Eq. (6) also indicates that f is proportional to the two-third power of R and inversely proportional to the one-third power of F_n. The nanofretting data presented in Fig. 9 were obtained with a sharp diamond indenter with $R=50$ μm and F_n ranging from 1 to 10 mN. On the other hand, asperities coming in contact in fretting tests with a GCr15 steel ball of $R=20$ mm range from nanoasperities to much larger asperities. Additionally, the total F_n in the fretting tests from 50 to 200 N distributes over many asperities in the multi-asperity contact. Considering all these factors, we can conclude from Eq. (6) that the friction coefficient f in this nanofretting is smaller than that in fretting.

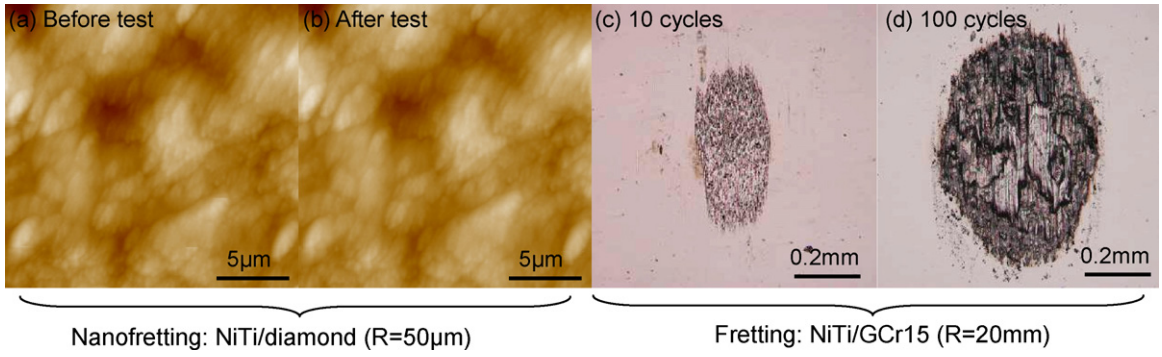

Fig. 10. AFM topography images of the wear area on NiTi (a) before and (b) after 50 cycles of nanofretting tests under the conditions (NiTi/diamond, $R=50$ μm) of $F_n=10$ mN and $D=500$ nm, compared with the optic images of the wear scars on NiTi under the fretting conditions (NiTi/GCr15, $R=20$ mm) of $F_n=100$ N and $D=50$ μm after (c) 10 cycles and (d) 100 cycles.

In addition, Fig. 9 also suggests that the f value of NiTi/diamond pair in nanofretting increases with the decrease in F_n at the same value of D, which is consistent with the prediction of Eq. (6). Nevertheless, for the multi-asperity contact of NiTi/GCr15 pair in fretting, the value of f is almost independent on the normal load.

To characterize the possible damage of NiTi surface in nanofretting, the AFM topography images were taken in the area before and after 50 cycles of nanofretting tests at the conditions of $F_n = 10$ mN and $D = 500$ nm. As shown in Fig. 10(a) and (b), no clear difference is found in the images before and after nanofretting tests. It is obviously different from the fretting tests at a similar Hertzian contact pressure, where the surface damage initiated in the first 10 fretting cycles and serious adhesive wear are found after 100 cycles of fretting in slip regime, as shown in Fig. 10(c) and (d). The reason can also be explained as the difference in the contact condition between nanofretting with single-asperity contact and fretting with multi-asperity contact. In nanofretting, the real contact area is close to the apparent Hertzian contact area. However, in fretting, the real contact area is much smaller than the apparent Hertzian contact area due to the fact of multi-asperity contact. The plastic deformation of asperities in contact will further induce the surface damage in fretting. Therefore, comparing to fretting, the low friction and near zero wear in nanofretting might be mainly attributed to the surface and size effects associated with unique operating conditions, such as improved mechanical properties of materials at the nano scale, small apparent contact area and single-asperity contact behavior.

4. Conclusions

With a triboindenter, the nanofretting of NiTi/diamond pair are performed under the tangential displacement amplitudes between 2 nm and 500 nm. Three typical nanofretting regimes of NiTi/diamond pair are observed under various normal loads and displacement amplitudes. Due to the surface and size effects, the nanofretting operates at different conditions from those of fretting and exhibits the following unique behaviors:

- With the increase in the number of nanofretting cycle, the maximum tangential force of NiTi/diamond pair almost keep constant in a nanofretting test, which is different from a fretting test of NiTi/GCr15 pair where the maximum tangential force shows a quick increase in the first dozens of cycles.
- The tangential stiffness of NiTi/diamond pair in nanofretting is about 2000 N/m, which is three orders magnitude smaller than that of NiTi/GCr15 pair in fretting.
- In slip regime, the friction coefficient of NiTi/diamond pair in nanofretting is between 0.09 and 0.12, which is about one-sixth of the values of f of NiTi/GCr15 pair in fretting.
- Accompanied with the low friction of NiTi/diamond pair in tangential nanofretting, no clear surface damage on NiTi is observed even after 50 cycles of nanofretting tests under a normal load of 10 mN.

Acknowledgements

The authors are grateful for the financial support from the Natural Science Foundation of China (50625515, 50575190, 50521503), the Research Grants Council of the Hong Kong SAR, China through Projects HKUST6199/03E and 619705, Specialized Research Fund for the Doctoral Program of Higher Education (20050613023), and the Program for New Century Excellent Talents in University (NCET-04-0887).

References

[1] Z.R. Zhou, L. Vincent, Fretting Wear, Science Press, Beijing, 2002.
[2] D. Dowson, History of Tribology, Professional Engineering Publishing Limited, London, 1998.
[3] Z.R. Zhou, L.M. Qian, Tribological size effect and related problems, Chin. J. Mech. Eng. 39 (2003) 22–26.
[4] S.M. Spearing, Materials issues in microelectromechanical systems (MEMS), Acta Mater. 48 (2000) 179.
[5] L.M. Qian, F. Tian, X.D. Xiao, Tribological properties of self-assembled monolayers and their substrates under various humid environments, Tribol. Lett. 15 (3) (2003) 169–176.
[6] P.J. Kennedy, M.B. Peterson, L. Stallings, An evaluation of fretting at small amplitudes, materials evaluation under fretting conditions, ASTM STP 780 (1982) 30–48.
[7] M. Varenberg, I. Etsion, G. Halperin, Nanoscale fretting wear study by scanning probe microscopy, Tribol. Lett. 18 (4) (2005) 493–498.
[8] H. Kahn, M.A. Huff, A.H. Heuer, The TiNi shape-memory alloy and its applications for MEMS, J. Micromech. Microeng. 8 (1998) 213–221.
[9] K.L. Ng, Q.P. Sun, Stress-induced phase transition and detwinning in NiTi polycrystalline shape memory alloy tubes, Mech. Mater. 38 (2006) 41–56.
[10] L.M. Qian, X.D. Xiao, Q.P. Sun, T.X. Yu, Anomalous relationship between hardness and wear properties of a superelastic nickel–titanium alloy, Appl. Phys. Lett. 84 (7) (2004) 1076–1078.
[11] L. Orgeas, D. Favier, Stress-induced martensitic transformation of a NiTi alloy in isothermal shear, tension and compression, Acta Mater. 46 (1998) 5579.
[12] L.M. Qian, Q.P. Sun, Z.R. Zhou, Fretting wear behavior of superelastic nickel titanium shape memory alloy, Tribol. Lett. 18 (4) (2005) 463–475.
[13] Z.R. Zhou, L. Vincent, Effect of external loading on wear maps of aluminum alloys, Wear 162–164 (1993) 619–623.
[14] K.L. Johnson, Contact Mechanics, Cambridge University Press, Cambridge, UK, 1985.
[15] B. Bhushan, Modern Tribology Handbook, Volume One, CRC Press LLC, FL, USA, 2001.
[16] Y. Berthier, Ch. Colombié, L. Vincent, M. Godet, Fretting wear mechanisms and their effects on fretting fatigue, J. Tribol. 7 (1988) 517.
[17] U.D. Schwarz, O. Zwörner, P. Köster, R. Wiesendanger, Quantitative analysis of the frictional properties of solid materials at low loads. I. Carbon compounds, Phys. Rev. B 56 (11) (1997) 6987–6996.
[18] W.D. Nix, H. Gao, Indentation size effects in crystalline materials: a law for strain gradient plasticity, J. Mech. Phys. Solids 46 (1998) 411.